Asteroids, Comets, Meteors
Proceedings IAU Symposium No. 229, 2005
D. Lazzaro, S. Ferraz-Mello & J.A. Fernández, eds.

doi:10.1017/S1743921305006721

What makes comets active?

Dina Prialnik

Department of Geophysics and Planetary Sciences, Tel Aviv University,
Ramat Aviv 69978, Israel
email: dina@planet.tau.ac.il

Abstract. There are three types of energy sources that affect comet nuclei and may render them active: thermal – solar radiation, nuclear – radioactive decay, and gravitational – through collisions and tidal forces. These sources give rise to processes that, in turn, may release, absorb or transport energy: sublimation or recondensation of volatiles, crystallization of amorphous ice, heat diffusion and advection, gas flow through the porous nucleus. Each of these sources and processes has its own characteristic time scale (or rate) and these may differ by many orders of magnitude. It is the competition between various processes and the interaction between them – as one triggers the other, or else impedes it – that determine the activity pattern and the internal structure of a comet nucleus. Examples of such interactions and their outcome are presented, such as apparently sporadic activity at large heliocentric distances, obtained from numerical simulations of the behavior and evolution of comet nuclei. Confrontation of modeling results with observations provides feedback and constraints for the assumptions and parameters on which models are based. Adjusting the latter to match observations reveals properties of the nucleus that are otherwise inaccessible (except for *in situ* measurements by space missions). However, the interpretation of observations, such as production rates in relation to nucleus abundances, may be misleading. It is shown that monitoring production rates over the active part of a periodic comet's orbit may lead to conclusions regarding the composition and structure of the nucleus.

Keywords. comets: general

1. Introduction

Whether comet nuclei contain pristine material, dating back to the time of formation of the solar system, cannot be directly probed; it has to be inferred by studying cometary activity. Comets are observed to be active in many different ways: outgasing of various species, the predominant one being H_2O; ejection of dust grains, ranging in size from submicron to centimeters; outbursts, that is, sudden surges of brightness and ejection of material, on a wide range of intensities and time scales; and occasionally, break-up of fragments or splitting of the nucleus. These are outward manifestations, observed and measured by increasingly sophisticated instruments and methods. Taken at face value, they should reveal the composition and structure of the nucleus. However, it is conceivable that the mechanisms responsible for cometary activity may have altered — at least to some extent — the structure of the nucleus as well. Therefore, the task of deducing the initial structure of the comet nucleus by observing its activity pattern is not a straightforward one. Only if we understand what makes comets active, may we hope to achieve the goal of determining the structure and composition of the nucleus at the time of comet formation.

Any type of cometary activity involves some energy source. These may be divided into primary (independent) and secondary (induced) sources. The dominant primary source is solar radiation, most of which is absorbed at the surface or in a surface layer [Davidsson & Skorov (2002)], since the albedo is relatively low. The important property of this source

is its strong dependence on heliocentric distance. Its effect depends on latitude, spin, and spin axis inclination [e.g., Cohen, Prialnik & Podolak (2003)]. Average heating rates may be used for processes that take place below the skin depth (see below). Another source, common in larger solar system bodies, is nuclear in nature and involves radioactive decay. Since comets are assumed to be initially homogeneous, this source is equally distributed over the volume. However, it mainly affects the deep interior of the nucleus, since the outer layers are efficiently cooled by emission of thermal radiation. Given the relatively slow supply of energy — even for short-lived radionuclides, such as ^{26}Al — the effect is a change in structure and composition [Prialnik & Podolak (1995), De Sanctis, Capria & Coradini (2001)], rather than enhanced activity. Energy input of gravitational origin is due to tidal forces exerted by large bodies (e.g., the sun or Jupiter), if a comet comes sufficiently close to them, or to occasional collisions. These are sporadic, of short duration, and rare.

Secondary sources — which may also be negative — are those connected with processes that are triggered by the primary sources, and include latent heat of phase transition, mostly sublimation, heat released in crystallization of amorphous water ice, and perhaps other sources associated with chemical reactions.

The evolution and activity of comets has been intensely studied in the last decade by several research groups through numerical modeling. Active modeler groups are listed below, keeping in mind that there is collaboration among groups or between members listed under different groups:

- M. J. S. Belton, N. H. Samarasinha, W. H. Julian...
- J. Benkhoff, W. F. Huebner, H. Rauer,...
- A. Coradini, M. T. Capria, C. De Sanctis, R. Orosei,...
- F. P. Fanale, J. R. Salvail, N. Bouziani,...
- J. Klinger, A. Enzian, S. Espinasse,...
- E. Kuehrt, H. U. Keller, N. I. Koemle, G. Kargl, Yu. Skorov, G. Steiner,...
- J. Leliwa-Kopystynski, K. J. Kossacki, W. J. Markiewicz,...
- D. Prialnik, M. Podolak, Y. Mekler, E. Beer, Y.-J. Choi, R. Merk, G. Sarid,...
- H. Rickman, B. J. R. Davidsson, M. J. Greenberg, P. J. Gutierrez, G. Tancredi,...
- L. M. Shulman, A. V. Ivanova,...
- T. Yamamoto, S. Sirono, A. Kouchi, S. Yabushita,...

An extensive review of modeling and results in all their aspects has been recently published [Prialnik, Benkhoff & Podolak (2005)]. Radiogenic heating and its effects have been studied by several groups as reviewed by [Merk & Prialnik (2003)] and it will not be addressed in this review. The effect of tidal forces was studied by Davidsson (2001).

In the following sections we shall focus on the link between the nucleus structure and the characteristics of cometary activity, in order to show how the latter can be used in order to deduce the former. Section 2 sets the scene for understanding the complex relations among processes that influence cometary activity, by analysing the characteristic time scales of these processes. Section 3 deals with the relation between production rates of various volatiles and their corresponding abundances in the nucleus. It uses, for illustration, models of comet 67P/Churyumov-Gerasimenko. Section 4 addresses the connection between the stratified structure of the outer layers of the nucleus and the variability of cometary activity, using models of comet 9P/Tempel 1 for illustration. The activity of this comet — continually monitored prior to the impact — was, indeed, observed to be variable [Meech *et al.* (2005)]. In Section 5 the possibility of outbursts in a distant comet is considered by means of an arbitrary comet model, which is evolved for a relatively long period of time (spanning hundreds of orbital revolutions). Conclusions are briefly summarized in Section 6.

2. Time scales

First, we briefly summarize the equations of evolution of a comet nucleus used — in one form or another — in all model calculations. Given the bulk mass density ρ and porosity Ψ, the equations of mass conservation for H_2O are

$$\frac{\partial \rho_a}{\partial t} = -\lambda \rho_a \,, \tag{2.1}$$

$$\frac{\partial \rho_c}{\partial t} = (1-f)\lambda \rho_a - q_v \,, \tag{2.2}$$

$$\frac{\partial \rho_v}{\partial t} + \nabla \cdot \mathbf{J}_v = q_v \,, \tag{2.3}$$

where the meaning of indices is: a – amorphous water ice, c – crystalline water ice, and v – water vapor; $\lambda(T) = 1.05 \times 10^{13} \mathrm{e}^{-5370/\mathrm{T}} \quad \mathrm{s}^{-1}$ is the rate of crystallization [Schmitt *et al.* (1989)], and f is the total fraction of occluded gas in amorphous ice. Similar equations hold for the other volatiles (α). The energy conservation — or heat diffusion — equation is

$$\sum_\alpha \rho_\alpha \frac{\partial u_\alpha}{\partial t} - \nabla \cdot (K \nabla T) + \left(\sum_\alpha c_\alpha \mathbf{J}_\alpha \right) \cdot \nabla T = \lambda \rho_a \mathcal{H}_{\mathrm{ac}} - \sum_\alpha q_\alpha \mathcal{H}_\alpha \,, \tag{2.4}$$

where $\mathcal{H}_{\mathrm{ac}}$ is the heat released upon crystallization, and $\mathcal{H}_\alpha$ is the heat of sublimation. The above set of time-dependent equations is subject to constitutive relations: $u(T)$, $\lambda(T)$, $q_\alpha(T, \Psi, r_p)$, $\mathbf{J}_\alpha(T, \Psi, r_p)$, $K(T, \Psi, r_p)$, where r_p denotes pore radius. These relations require additional assumptions for modeling the structure of the nucleus.

The rate of sublimation — mass per unit volume of cometary material per unit time — is given by

$$q_\alpha = S(\Psi, r_p) \left[(P_{\mathrm{vap},\alpha}(T) - P_\alpha) \sqrt{\frac{\mu_\alpha}{2\pi R_g T}} \right] , \tag{2.5}$$

where the term in square brackets represents the sublimation rate per unit surface area, and S is the surface to volume ratio, a function of porosity and pore radius. The partial pressure P_α is given by the ideal gas law and the saturated vapor pressure, P_{vap}, by the Clausius – Clapeyron approximation,

$$P_{\mathrm{vap}}(T) \;=\; A \mathrm{e}^{-B/T} \,. \tag{2.6}$$

where A and B are constants.

The equations of mass conservation and energy transport require two boundary conditions each: at the center of the nucleus, vanishing (a) heat flux and (b) mass (gas) fluxes; at the surface, (c) energy balance,

$$F(R) = \epsilon \sigma T(R,t)^4 \;+\; \mathcal{F} P_{\mathrm{vap}}(T) \sqrt{\frac{\mu}{2\pi R_g T}} \mathcal{H} \;-\; (1-\mathcal{A}) \frac{L_\odot}{4\pi d_H(t)^2} \cos z \,, \tag{2.7}$$

where z is the solar zenith angle, and $\mathcal{F} \leqslant 1$ represents the fractional area of exposed ice — since the surface material is a mixture of ice and dust [Crifo & Rodionov (1997)] — and (d) gas pressures exerted by the coma, which — in the lowest approximation — may be assumed to vanish.

Dust is assumed to be, in part, dragged along with the gas flowing through pores and, in part, lifted off the nucleus surface by the sublimating vapor [see Orosei *et al.* (1995)]. For the former, the dust velocity is assumed to be equal to the gas velocity [see Podolak & Prialnik (1996)]. An efficiency factor is calculated, to take account of a dust size distribution that allows only grains up to a critical size to be dragged or lifted off.

https://doi.org/10.1017/S1743921305006721 Published online by Cambridge University Press

The rest may accumulate to form a dust mantle. The efficiency factor may be adjusted so as to allow or prevent the formation of a sealing mantle.

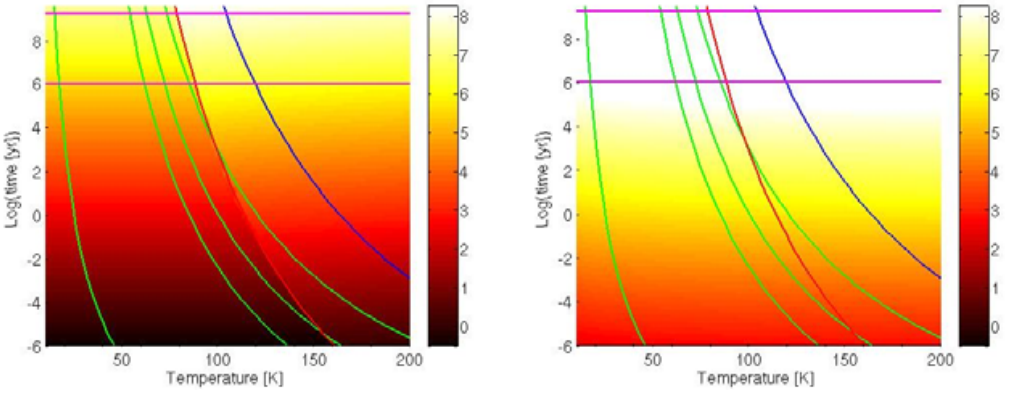

Figure 1. Characteristic times cales of various processes as function of temperature. The depth scale of diffusion is mapped onto the [temperature, diffusion time] plane. The left panel corresponds to heat diffusion, the right – to vapor diffusion. A sharp shift occurs along the curve corresponding to the H_2O crystallization time scale. The other curves represent sublimation time scales for: CO, CO_2, NH_3, HCN and H_2O, from left to right, in order of decreasing volatility. The horizontal lines are the characteristic decay times of ^{26}Al, and above it, ^{40}K.

The evolution of a comet is determined by several different time scales:

• The thermal time scale, obtained from the energy balance equation, which in its simplest form, without sources and advection, is a heat diffusion equation. Distinction must be made between the thermal time scale of amorphous ice τ_a, crystalline ice τ_c, and dust τ_d. For a layer of thickness Δr and average temperature T we have:

$$\tau_a(\Delta r,\, T) = (\Delta r)^2 \rho_a c_a / K_a(T), \tag{2.8}$$

and similar expressions for τ_c and τ_d.

• The time scale of gas diffusion (say, for some representative gas component) τ_{gas}, which is also the time scale of pressure release, obtained from the mass conservation equation, which (without sources) can be regarded as a diffusion-type equation for the release of gas pressure.

$$\tau_{gas}(\Delta r,\, T) = \frac{3}{4}\frac{(\Delta r)^2}{pa}\left(\frac{2\pi\mu}{kT}\right)^{1/2} \tag{2.9}$$

• The time scale of crystallization τ_{ac}, which is also the time scale of gas-release and pressure build-up,

$$\tau_{ac}(T) = \lambda(T)^{-1} = 9.54 \times 10^{-14} e^{5370/T} \qquad \text{sec} \tag{2.10}$$

• The time scales of sublimation of the different volatiles, $\tau_{sub-\mathrm{H_2O}}$ for water, $\tau_{sub-\mathrm{CO}}$ for CO, $\tau_{sub-\mathrm{CO_2}}$ for CO_2, and so forth.

$$\tau_{sub-\mathrm{H_2O}}(T) = \frac{\rho_c}{S\mathcal{P}_v\sqrt{\mu_v/2\pi R_g T}}, \tag{2.11}$$

and similar expressions for other volatiles.

To these, the constant characteristic times of decay of the radioactive species may be added; the only relevant one would be that of ^{26}Al, whose decay time τ_{Al26} is relatively short.

https://doi.org/10.1017/S1743921305006721 Published online by Cambridge University Press

All these time scales are shown in Figure 1 as function of temperature. The background is a map of the length (depth) scale corresponding to a given diffusion time scale and temperature, since diffusion time scales (for heat and gas) depend on length. We consider two cases: heat diffusion and advective diffusion of a representative gas. In the former, we note a sharp change of depth where ice transforms from amorphous to crystalline, illustrating the fact that crystalline ice is a much better heat conductor than amorphous ice. The change occurs along the curve representing the time scale of crystallization as a function of temperature. The other curves in Fig. 1 represent the sublimation time scales for various volatiles: CO, CO_2, NH_3, HCN and H_2O, in order of increasing time, that is, decreasing volatility.

The relationships between these time scales will determine to a large extent the evolutionary pattern of the comet nucleus. For example, considering the time scales of crystallization, sublimation and heat conduction, we find that at very low temperatures conduction dominates on the relevant length scales, meaning that heat released by a local source will be efficiently removed. Crystalline ice is a much better heat conductor than amorphous ice and hence heat will predominantly flow to the surface through the growing outer crystalline layer. As the crystallization rate is much more sensitive to temperature than the conduction rate (of crystalline ice), it will, eventually surpass the rate of heat conduction. When, due to insolation, the temperature at the crystallization front reaches this critical temperature $T_c \sim 120$ K, the local heat release causes it to rise still further. The higher temperature causes crystallization to proceed even faster and thus a runaway process develops. As the temperature rises, sublimation of the ice from the pore walls becomes important and since it absorbs a large amount of energy per unit mass, the outburst is arrested and proceeds at a controlled steady-state rate.

The time scale of gas diffusion is also characteristic of pressure release. Thus, if gas is released in the interior of the nucleus — due to crystallization of gas-laden amorphous ice or to sublimation — at a depth that surpasses the diffusion length scale (shown in Fig. 1), pressure may build up beyond the material strength and thus breaking and outbursts may result. The critical depth depends on temperature and on the active gas species and hence the outcome of gas release will depend on heliocentric distance and nucleus structure and history.

We note, in particular, that the sublimation curve of HCN intersects the crystallization curve at a temperature slightly above 100 K, where both processes proceed at a characteristic time scale of a few hundred years. At a depth of about 100 m, conduction competes with them, while at a larger depth conduction will be negligible. We shall return to this point when discussing outbursts at large heliocentric distances.

3. From production rates to nucleus composition

A comet nucleus is expected to include many different volatile species, such as are observed in the coma. If cometary water ice is crystalline, these volatiles will be frozen out as separate phases; if cometary ice is amorphous, volatiles may be trapped in the amorphous ice. In the former case, as the heat absorbed at the surface penetrates inward, ices other than water will evaporate and the gas will flow, in part, to the surface and out of the nucleus, and in part, to the colder interior, where it will refreeze. Since evaporation rates are strongly temperature dependent and vary widely among gas species, several distinct evaporation fronts are expected to form, and also several separate layers of refrozen gases (although initially, the ice mixture may have been homogeneous). These layers will evaporate, in turn, when erosion of the nucleus will bring them closer to the

https://doi.org/10.1017/S1743921305006721 Published online by Cambridge University Press

surface. Hence, the layered structure may move toward the center, but at the same time remain constant in depth relative to the surface.

Properties of 5 different species are summarized in Table 3. Constants A and B correspond to the coefficients of the Clausius-Clapeyron approximation to the saturated vapor pressure (2.6); they also serve to calculate the typical sublimation temperature,

$$T_s = B/\ln(A/\text{const}). \tag{3.1}$$

The rate of advance of the sublimation front $\dot{z}$ into the nucleus is then estimated for each species by assuming that the conduction flux inward from the surface (typically of order 100W m^{-2}) is absorbed solely in the evaporation of that species,

$$\frac{dz}{dt} = \frac{F_{in}}{\rho X_{ice}\mathcal{H}}. \tag{3.2}$$

Table 1. Volatile properties

Ice	A 10^{10}Nm^{-2}	B K	T_s K	$\mathcal{H}$ 10^6J kg^{-1}	dz/dt cm/d
H_2O	356.	6141.67	133	2.83	0.8
HCN	3.8665	4024.66	97	1.24	37
NH_3	61.412	3603.6	81	1.76	26
CO_2	107.9	3148.	70	0.594	78
CH_4	0.597	1190.2	30	0.617	75
CO	0.1263	764.16	20	0.227	200

If gas is trapped in amorphous ice, it will first escape when the ice crystallizes. It is implied that several gas species can be simultaneously trapped in amorphous ice, and that these gases are released from the ice upon crystallization regardless of their properties (and these assumptions warrant further investigation by laboratory experiments). Thus first, all species will escape together, and secondly, they will escape, generally, at higher temperatures than those typical of evaporation. Once they are released from the ice, these gases will behave similarly to gases that evaporate from the pore walls, flowing in part toward the surface and, in part, toward the interior. In this case, too, a layered structure of refrozen volatiles will emerge, and will eventually evaporate at a later stage. We shall return to this characteristic structure of multi-component nuclei in Section 4.

It has long been recognized that production rates of different volatiles ejected by an active comet should not be taken to reflect the corresponding abundances in the nucleus, as determined at the time of comet formation [e.g., Benkhoff & Huebner (1995)], and thus abundaince ratios in the coma may be vastly different from those of the nucleus, even before molecules are processed by solar radiation. If the source of volatiles is sublimation of the icy phase in the interior of the nucleus, the different rates of outgasing are the direct consequence of the differences in volatility, that is, sublimation temperature and latent heat. In addition, the mobility of the molecules that have to diffuse to the surface is also different. But even if the gases are trapped in amorphous ice and released upon crystallization, in which case they are presumably released in the same proportion, this proportion is not preserved all the way to the surface of the nucleus. The reason, as stated above, is that a fraction of the gas flows inward, refreezes behind the crystallization front and may sublimate later on, independently of crystallization.

https://doi.org/10.1017/S1743921305006721 Published online by Cambridge University Press

This complex behavior is expected to result in production rates that are individual to each species. In order to test this inference and asses the extent of the discrepancy between ejecta and nucleus compositions, several models have been calculated, adopting the characteristic parameters of comet 67P/Churyumov-Gerasimenko, listed in Table 2 below. The compositions adopted for the different models (labelled 1 to 5) are listed in

Table 2. Parameters for comet 67P/Churyumov-Gerasimenko models

Property	Value
Semi-major axis	3.507 AU
Eccentricity	0.6316
Spin period	12.69 hr
Radius	1.98 km
Bulk density	500 kg m^{-3}

Table 3. It includes three types of volatile mixtures: amorphous water ice and trapped gases, crystalline water ice mixed with ices of other volatiles, as well as a combined composition of amorphous water ice and trapped gases mixed with ices of the same species.

Table 3. Initial volatile abundances: first row – frozen; second row – trapped in amorphous ice

Model (T_0)	X_d	$X_{\rm ice}$	CO	CO_2	CH_4	HCN	NH_3
1.(50 K)	0.50	0.50	—	—	—	—	—
		am	5%	2%	1%	1%	1%
2.(50 K)	0.20	0.80	—	—	—	—	—
		am	5%	2%	1%	1%	1%
3.(50 K)	0.20	0.71	—	0.03	—	0.03	0.03
		am	5%	2%	1%	1%	1%
4.(20 K)	0.25	0.60	0.03	0.03	0.03	0.03	0.03
		cr	—	—	—	—	—
5.(40 K)	0.25	0.60	0.03	0.03	0.03	0.03	0.03
		cr	—	—	—	—	—

Models were run for 6 to 9 consecutive orbits and the resulting production rates and production rate ratios compared to corresponding initial abundance ratios in the nucleus are shown in Figures 2 and 3. Considering ratios of production rates has the advantage that some of the arbitrariness inherent in modeling is thus eliminated. We note that volatile ratios in the ejecta may differ from the corresponding ones in the nucleus by as much as a factor of 100! A noteworthy exception is the ratio CO/CH_4, which involves two supervolatile species. These species remain in gaseous form throughout the nucleus, and retain their relative abundances. We also note that the ratios of volatiles do not remain constant, but change along the orbit. If we now integrate production rates over time to obtain the total amount of material ejected during one orbit for each species and then compare ratios of these amounts with the ratios of abundances of the same species in the nucleus, a completely different picture emerges: not only are the differences far smaller, but they converge with repeated orbital revolutions to values which are very closely representative of the nucleus abundance ratios. This is illustrated in Figure 4.

https://doi.org/10.1017/S1743921305006721 Published online by Cambridge University Press

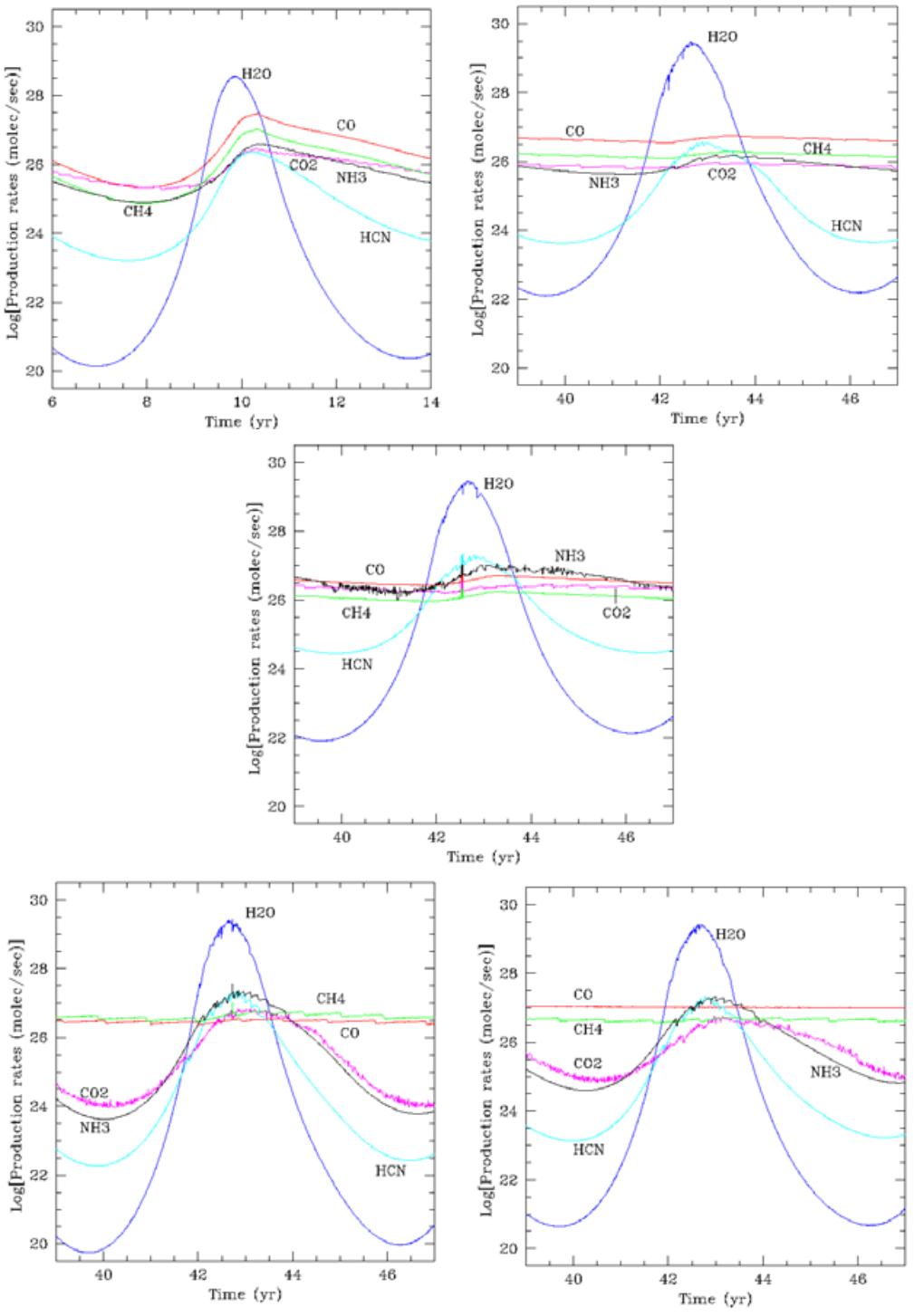

Figure 2. Production rates for one orbital revolution for the models of comet 67P/Churyumov-Gerasimenko as listed in Table 3: 1–top left, 2–top right, 3–middle, 4–bottom left, and 5–bottom right.

https://doi.org/10.1017/S1743921305006721 Published online by Cambridge University Press

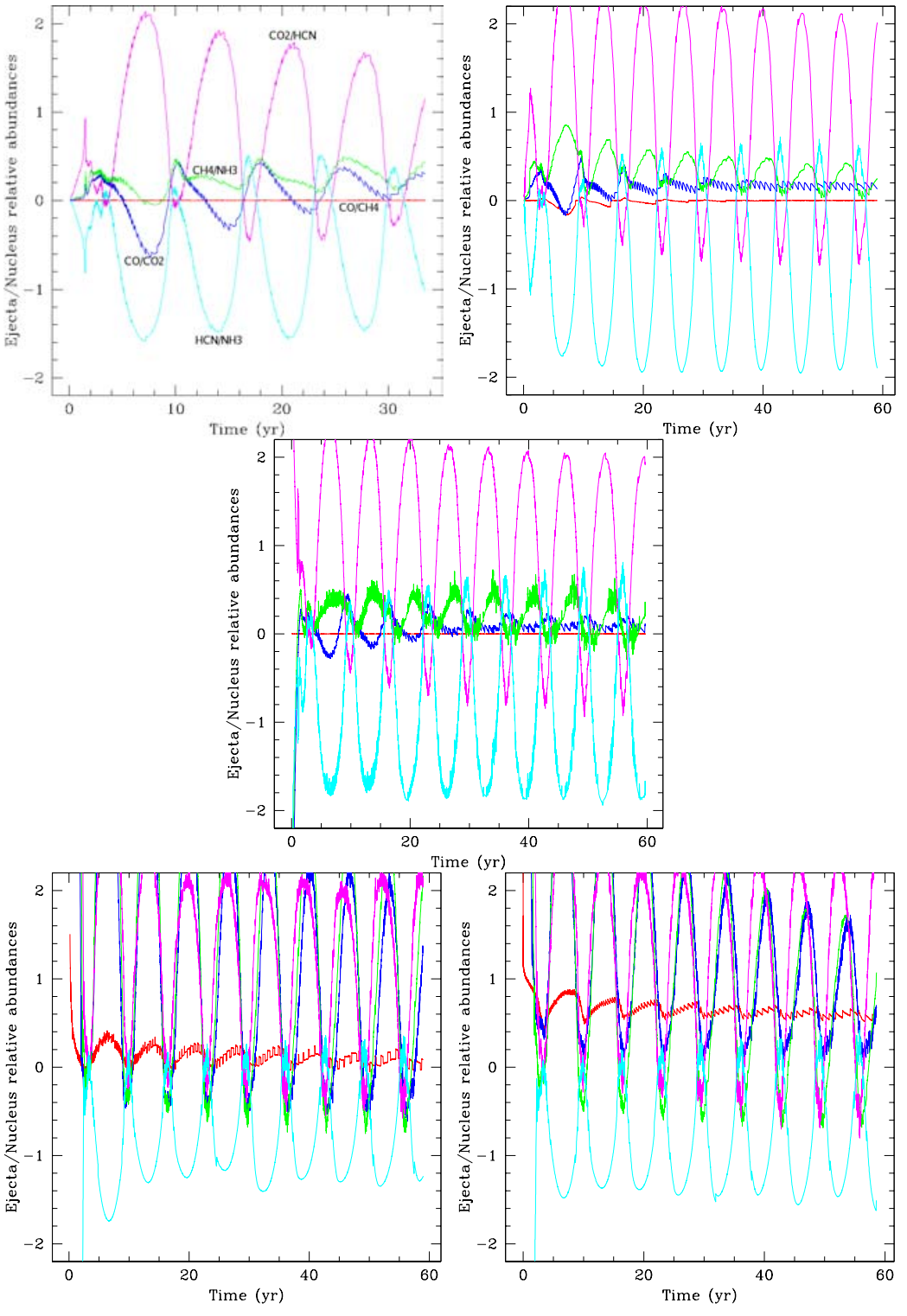

Figure 3. Abundance ratios in the ejecta relative to initial abundance ratio (log scale) as a function of time, along several orbital revolutions for the models listed in Table 3: 1 (top left), 2 (top right), 3 (middle), 4 (bottom left), and 5 (bottom right). Curves are labelled for model 1 (in the color version: blue $CO\,/\,CO_2$; green $CH_4\,/\,NH_3$; cyan $HCN\,/\,NH_3$; magenta $CO_2\,/\,HCN$; red $CO\,/\,CH_4$); results for the other models serve to illustrate the large ratios obtained and the wide variability among species.

https://doi.org/10.1017/S1743921305006721 Published online by Cambridge University Press

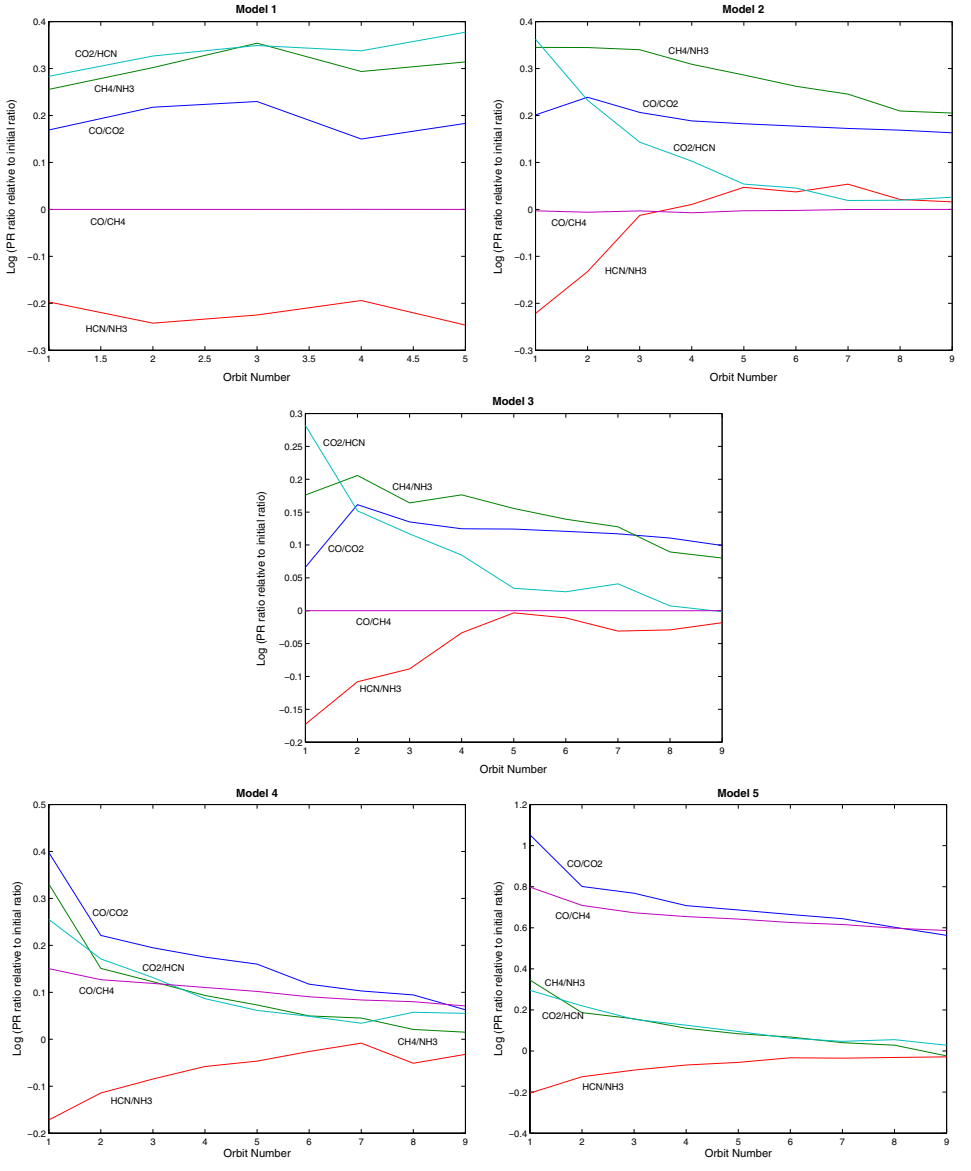

Figure 4. Abundance ratios — obtained by integrating the corresponding production rates over a full orbital revolution — relative to initial abundance ratios in the nucleus (log scale) for several consecutive orbits for the models listed in Table 3: 1 (top left), 2 (top right), 3 (middle), 4 (bottom left, and 5 (bottom right).

This result is of great significance to observations of production rates. It means that if a comet is monitored for a sufficiently large portion of its orbit (where it is highly active) and the obtained production rates are then integrated over that time, the resulting relative abundances should be far closer to those prevailing in the nucleus than they would be at any given point of the orbit. Therefore, continuous observation of a comet (within limits and constraints) are strongly indicated.

https://doi.org/10.1017/S1743921305006721 Published online by Cambridge University Press

4. Variable activity and stratified nucleus structure

Although solar energy is supplied as a smooth function of heliocentric distance, the activity of a comet — as it approaches and then moves away from the sun — is not. The rate of outgasing and dust emission is typically variable, and often outbursts are observed. The most recent and detailed evidence to this variability has been provided by the extensive observations of comet 9P/Tempel 1, the target of the *Deep Impact* mission (Meech *et al.* 2005), but the same behavior was exhibited, for another example, by comet Hale-Bopp [Biver *et al.* (2002)]. In order to understand the variability in outgasing and dust emission, we consider the numerical model calculated by Sarid *et al.* (2005) for this comet. The model assumes a porous, spherical and initially homogeneous nucleus composed of amorphous and crystalline water ice, dust, and 5 other volatile species: CO, CO_2, HCN, NH_3, and C_2H_2. The basic comet nucleus code [Prialnik (1992)] is the same as that used for the calculations described in Section 3 for comet 67P/C-G. In addition, this calculation takes into account rotation of the nucleus and latitudinal variation of insolation. Relevant parameters are listed in Table 4. Structural and compositional parameters were chosen so as to match measured production rates at several points on the orbit [Cochran *et al.* (1992), Osip, Schleicher & Millis (1992)].

Table 4. Parameters for comet 9P/Tempel 1 model

Property	Value
Semi-major axis	3.12 AU
Eccentricity	0.517491
Spin period	41.85 hr
Radius	3.3 km
Bulk density	500 kg m^{-3}
Dust mass fraction	0.5
Ice (a) mass fraction	0.5

The outstanding feature emerging from this calculation is the complicated stratification pattern as a function of depth, where layers enriched in various volatiles alternate. Moreover, several layers enriched in the same volatile may appear at different depths. The effect is illustrated by the mass fraction of amorphous ice and of various volatiles shown in Figure 5.

We recall that the model's composition includes 5 volatile species trapped in amorphous water ice. These volatiles cover a wide range of sublimation temperatures (see Table 3). As the surface of the nucleus is heated and the heat wave propagates inward, the amorphous ice crystallizes and the trapped gas is released. The gas pressure in the pores peaks at the crystallization front. As a result (and as already mentioned earlier), gas flows in part outward and escapes, and in part, inward into colder regions. Eventually, each species reaches a sufficiently cold region for it to recondense. Since recondensation releases heat, it affects the composition of its surroundings and thus a complicated pattern results, of alternating ices mixed with the amorphous water ice. When another heat wave reaches these regions, on a subsequent perihelion passage, the heat is absorbed in sublimation of the recondensed volatiles rather than in crystallization of amorphous ice. This is how alternating layers of crystalline and amorphous ice arise, rather than a single boundary between a crystalline exterior and an amorphous interior.

The stratified layer extends from a depth of about 10 m below the surface and down to a few hundred meters. Since 10 m is roughly the orbital skin depth for 9P/Tempel 1,

https://doi.org/10.1017/S1743921305006721 Published online by Cambridge University Press

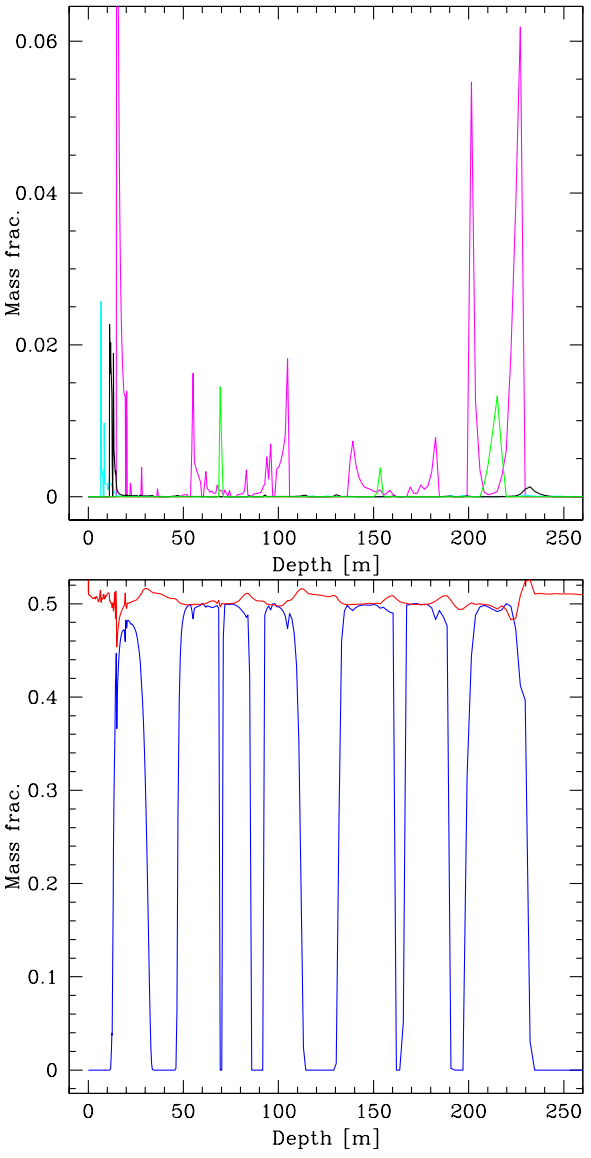

Figure 5. A model of Comet 9P/Tempel 1, near perihelion. *Top* – mass fractions of volatile ices as a function of depth: the outermost peak is HCN, followed by NH_3 and CO_2, then between each two CO_2 peaks there is a lower peak of C_2H_2. *Bottom* – amorphous H_2O ice (oscillating curve) and dust (upper curve) as a function of depth.

this structure should cause activity variations on the orbital time scale. This means that activity may differ from orbit to orbit and occasional spurious outbursts may arise, when the heat wave propagating down from the surface reaches a region enriched in ice of some volatile species. Such outbursts of gas should be accompanied by ejection of dust. Indeed, this variable behavior is apparent in Figure 6, where production rates for all volatiles are shown as function of time, pre- and post-perihelion. Besides the variability encountered for each gas species, we note the marked differences among production rates of different volatiles (similar to the results obtained for comet 67P/C-G, see Section 3). Thus

https://doi.org/10.1017/S1743921305006721 Published online by Cambridge University Press

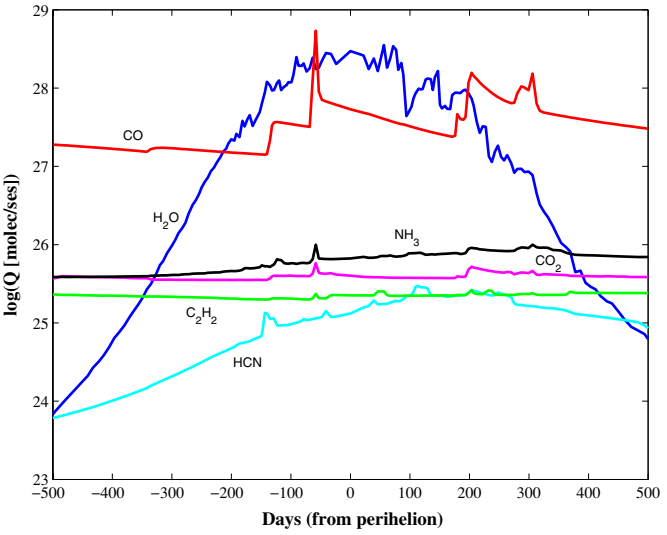

Figure 6. Production rates of volatiles as a function of time measured from perihelion obtained for a model of Comet 9P/Tempel 1.

variability in cometary activity is easily explained. It should be mentioned, however, that the details of the computation results depend on assumptions and adopted parameters. The important theoretical result is the variability *itself*, its general pattern, and the typical amplitude and time scale ranges.

Production rates are shown in more detail in Figure 7, where they are plotted separately, in order of volatility. Changes amounting to factors of up to 5 in outgasing rates can thus be discerned. Since the temperature profile of the nucleus is a decreasing function of depth, the stratified structure follows the inverse order of volatility, with the most volatile species lying deepest, and the least volatile closest to the surface. It is noteworthy that the departure from correlation with heliocentric distance is clearly dependent on volatility. Water production is the most strongly and directly correlated to solar heating, since H_2O sublimates mostly from the surface or a thin subsurface layer. Thus water production is closely correlated with the change in surface temperature, illustrated in Figure 8-left. The next two species in order of volatility, HCN and NH_3, sublimate from correspondingly deeper layers, which have become enriched in these volatiles due to recondensation of trapped gas. However, both these layers are found within the orbital skin depth, and are hence correlated with solar heating. In addition, we discern a shift in time of the evaporation rate peak. This is due to the thermal lag of the heat front propagating inward from the surface. The more volatile species, C_2H_2 and CO, originate in deeper layers, or are entirely released from amorphous ice, and therefore their production rates are completely independent of the time variation of solar heat. Finally, the right panel of Fig. 8 shows the dust production rate, which reflects the high variability of the total gas production, since dust is dragged by the gas.

5. Distant outbursts and amorphous water ice

The possibility of a comet being active at large heliocentric distances is now illustrated, based on long-term evolutionary calculations, assuming an arbitrary orbit of low

https://doi.org/10.1017/S1743921305006721 Published online by Cambridge University Press

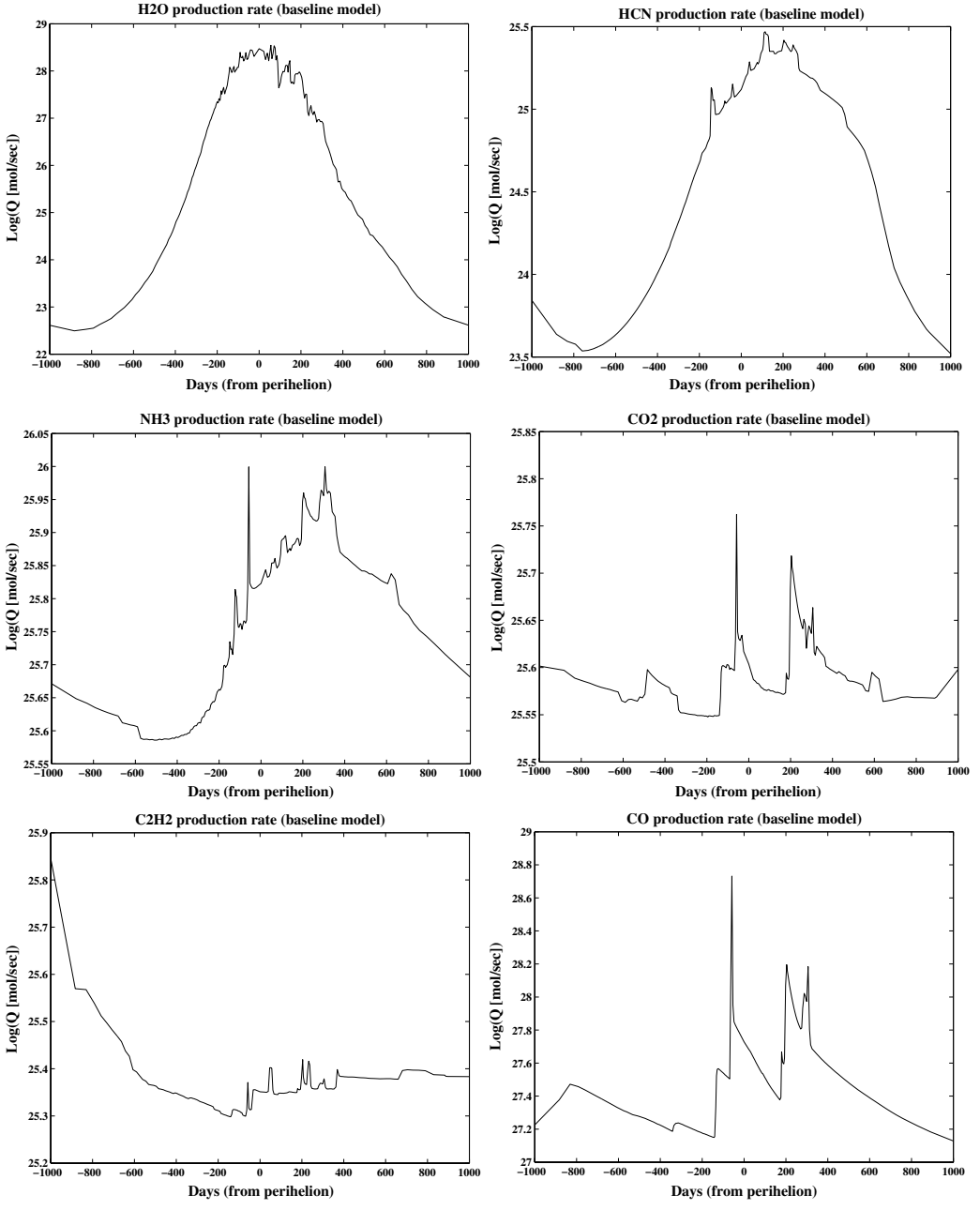

Figure 7. Production rates of various volatiles (see Fig. 6) as a function of time measured from perihelion, as obtained for a model of Comet 9P/Tempel 1: *top left* - H_2O; *top right* - HCN; *middle left* - NH_3; *middle right* - CO_2; *bottom left* - C_2H_2; *bottom right* - CO.

eccentricity, with a semimajor axis of 23 AU, and a composition of amorphous ice and 5 volatile species — as in Section 3 — trapped in it [from Choi (2005)]. Solar radiation is still the primary energy source, but it mainly serves to ignite other, secondary sources. The temperature at the sub-solar point reaches above 100 K, at which point crystallization is triggered and the trapped gases are released from the ice. A new heat wave

https://doi.org/10.1017/S1743921305006721 Published online by Cambridge University Press

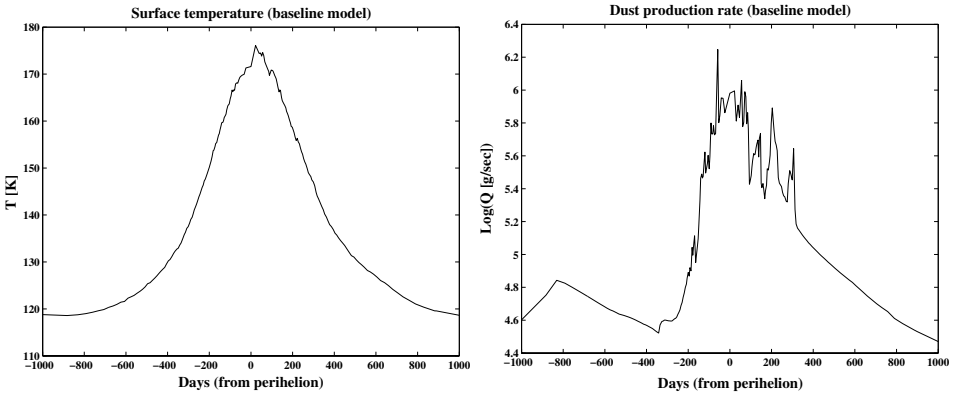

Figure 8. Surface temperature at subsolar point (left) and dust production rate (right) obtained for a model of Comet 9P/Tempel 1.

propagates inward from the surface at the perihelion of each orbit, and thus crystallization is supported by the energy of the heat wave at each perihelion passage, but proceeds extremely slowly. A non-negligible amount of volatile gases is released near perihelion at each orbit, but given the large distance, this activity would remain below detection limit. The moderately volatile gases (CO_2, NH_3 and HCN) recondense — in part — at depths of tens of meters, while the highly volatile ones (CO and CH_4) entirely escape from the nucleus. This is the same effect encountered earlier. Figure 9-top shows the evolution of gas production rates.

After a few tens of orbits a very strong outburst occurs. It arises due to a finely-tuned interaction between recondensation of volatiles and crystallization of amorphous ice on the same time scale (note the intersection of the phase transition times cale of HCN and the crystallization time scale in Fig. 1). As the moderately volatile gases released upon crystallization flow inward into colder regions of the nucleus, recondense and release latent heat, the local temperature rises to the critical value of $\sim$ 100 K. Thus a new crystallization wave is triggered at the densest region of recondensed ice, below the old crystallization front. Crystallization, in turn, releases more heat and occluded gas. For a very brief period of time, in a narrow region, the temperature shoots up to almost 200 K, as shown in the middle panel of Fig. 9. This is close to the maximal temperature reached by the ice on the surface of a comet nucleus near the sun, when sublimation prevents the temperature from rising further. Indeed, the heat of crystallization causes the recondensed ice to sublimate and thus the outburst is due to all the volatile gases: those released by the new crystallization episode as well as those sublimated from recondensed volatile ices by absorption of the crystallization energy. This type of interaction also occurred in the models described in Section 4 and produced variable abundance profiles and short-term, low-amplitude outbursts.

A second outburst, less strong in terms of gas production, but of much longer duration (in fact, a long period of high activity, rather than an outburst), occurs after a large number of quiet orbital revolutions. It originates at a larger depth below the nucleus surface, as shown in the lowest panel of Fig. 9, and involves slow crystallization down to a depth of almost 300 m below the surface. Thereafter the interior cools down and the highest temperature is again obtained at the surface.

It is interesting to consider the possibility of repetitive outbursts. The phase transition time scale of moderately volatile gases is comparable with the diffusion time scale through the orbital skin depth, as shown in Figure 1. Therefore, this kind of outburst may not

https://doi.org/10.1017/S1743921305006721 Published online by Cambridge University Press

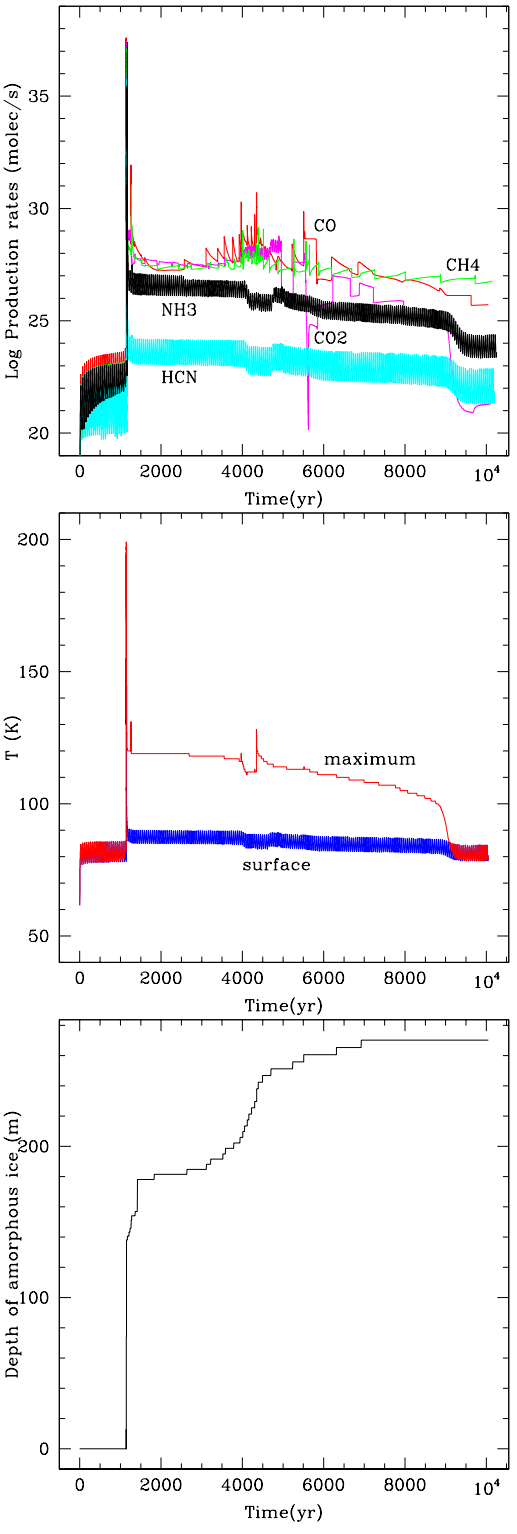

Figure 9. Long-time evolution of a distant comet: *top:* volatile production rates; *middle* maximal temperature and surface temperature; *bottom:* depth of amorphous ice boundary.

https://doi.org/10.1017/S1743921305006721 Published online by Cambridge University Press

be repetitive. It would be only if the nucleus surface receded due to sublimation — as in short-period comets — but this effect is negligible for the orbit of a distant object. A change of orbit, however, could trigger new outbursts.

6. Conclusions

The activity of a comet nucleus, as predicted by numerical model computations, is variable on different scales, from frequent low-amplitude outbursts, to major outbursts that may be observed at large heliocentric distances. This pattern of behavior results from the inhomogeneity inherent to the outer layers of the nucleus, extending down to possibly a few hundred meters below the surface. The composition of these layers is stratified, with alternating layers enriched in different volatiles. Given that the the characteristic pattern of activity of a comet is determined to a large extent by the structure of the nucleus, it should be possible to use observations of production rates in order to deduce properties of the nucleus interior.

Thus, we have shown that integrated production rate ratios can be used to derive the corresponding abundance ratios of the nucleus composition. Fluctuations in production rates can be used to infer a stratified structure of the outer layers of the nucleus. Furthermore, they may indicate whether the water ice is amorphous or crystalline, or mixed. The systematic differences in production rate dependence on heliocentric distance for various volatiles may, perhaps, be used to get a rough estimate of the relative depths below the nucleus surface where these species originate. We are still far from fully understanding the elusive nature of comet nuclei, but these findings may guide us towards achieving this goal by close collaboration between observations and modeling.

Acknowledgements

I would like to thank Fanny Gur and Gal Sarid for their help with model computations and analysis of the data. Support for this work was provided by Israel Science Foundation grant No.942/04.

References

Benkhoff, J. & Huebner, W.F. 1995, *Icarus* 114, 348
Benkhoff, J. & Boice, D.C. 1996, *Planet. Space Sci.* 47, 665
Biver, N., & 21 collaborators. 2002, *Earth, Moon & Planets* 90, 5
Bouziani, N. & Fanale, F.P. 1998, *Astrophys. J.* 499, 463
Capria, M.T., Capaccioni, A., De Sanctis, M.C., Espinasse, S., Federico, C., Orosei, R., & Salomone, M. 1996, *Planet. Space Sci.* 44, 987
Capria, M.T., Coradini, A., & De Sanctis, M.C. 2002, *Earth Moon & Planets* 90, 217
Capria, M.T., Coradini, A., De Sanctis, M.C., & Orosei, R. 2000, *Astron. J.* 119, 3112
Choi, Y.-J. 2005, PhD thesis, Tel Aviv University, Tel Aviv
Choi, Y.-J., Cohen, M., Merk, R., & Prialnik, D. 2003, *Icarus*
Cochran, A.L., Barker, E.S., Ramseyer, T.F., & Storrs, A.D. 1992, *Icarus* 98, 151
Cohen, M., Prialnik, D., & Podolak, M. 2003, *New Astron.* 8, 179
Coradini, A., Capaccioni, A., Capria, M.T., De Sanctis, M.C., Espinasse, S., Federico, C., Orosei, R., & Salomone, M. 1997, *Icarus* 129, 317
Crifo, J.F. & Rodionov, A.V. 1997, *Icarus* 129, 72
Davidsson, B.J.R. 1999, *Icarus* 142, 525
Davidsson, B.J.R. 2001, *Icarus* 149, 375
Davidsson, B.J.R. & Skorov, Yu.V. 2002, *Icarus* 159, 239
Davidsson, B.J.R. & Skorov, Yu.V. 2004, *Icarus* 168, 163
De Sanctis, M.C., Capria, M.T., & Coradini, A. 2001, *Astron. J.* 121, 2792

Enzian, A., Klinger, J., Schwehm, G., & Weissman, P.R. 1999, *Icarus* 138, 74
Fanale, F. & Salvail, J.R. 1997, *Icarus* 125, 397
Greenberg, J.M., Mizutani, H., & Yamamoto, T. 1995, *Astron.& Astrophys* 295, L35
Gutirrez, P.J., Ortiz, J.L, Rodrigo, R., & Lopez-Moreno, J.J. 2000, *Astron.& Astrophys* 355, 809
Huebner, W.F., Benkhoff, J., Capria, M.T., Coradini, A., De Sanctis, C., Enzian, A., Orosei, R., & Prialnik, D. 1999, *Adv. Space res* 23, 1283
Ivanova, A. & Shulman, L. 2002, *Earth Moon & Planets* 90, 249
Julian, W.H., Samarasinha, N.H., & Belton, M.J.S. 2000, *Icarus* 144, 160
Klinger, J., Levasseur-Regourd, A.C., Bouziani, N., & Enzian, A. 1996, *Planet.& Space Sci.* 44, 637
Kossacki, K.J., Szutowicz, S., & Leliwa-Kopystynski, J. 1999, *Icarus* 142, 202
Kuehrt, E. 2002, *Earth Moon & Planets* 90, 61
Meech, K.J, A'Hearn, M.F., Fernández, Y.R., Lisse, C.M., Weaver, H.A., Biver, N., & Woodney, L.M. 2005, *Space Sci. Rev.* 117, 297
Merk, R. & Prialnik, D. 2003, *Earth, Moon & Planets* 92, 359
Orosei, R., Capaccioni, F., Capria, M.T., Coradini, A., Espinasse, S., Federico, C., Salomone, M., & Schwehm, G.H. 1995, *Astron.& Astrophys* 301, 613
Osip, D.J., Schleicher, D.G., & Millis, R.L. 1992, *Icarus* 98, 115
Podolak, M. & Prialnik, D. 1996, *Planet.& Space Sci.* 44, 655
Prialnik, D. 1992, *ApJ* 388, 196
Prialnik, D. 1999, *Earth Moon & Planets* 77, 223
Prialnik, D., Benkhoff, J., & Podolak, M. 2005, in: M. Festou *et al.* (eds.), *Comets II* (Tucson: Univ. Arizona Press), p 359
Prialnik, D. & Podolak, M. 1995, *Icarus* 117, 420
Sarid, G., Prialnik, D., Meech, K.J., Pittichova, J., & Farnham, T. 2005, *Publ. Astron. Soc. Japan* 117, 796
Schmitt, B., Espinasse, S., Grim, R. J. A., Greenberg, J. M., & Klinger, J. 1989, *ESA SP* 302, 65
Shoshany, Y., Heifetz, E., Prialnik, D., & Podolak, M. 1997, *Icarus* 126, 342
Shoshany, Y., Podolak, M., & Prialnik, D. 1999, *Icarus* 137, 348
Shoshany, Y., Prialnik, D., & Podolak, M. 2002, *Icarus* 157, 219
Sirono, S. & Greenberg, J.M. 2000, *Icarus* 145, 230
Sirono, S. & Yamamoto, T. 1997, *Planet.& Space Sci.* 45, 827
Skorov, Yu.V., Keller, H.U., Jorda, L., & Davidson, B.J.R. 2002, *Earth Moon & Planets* 90, 293
Skorov, Yu.V. & Rickman, H. 1998, *Planet.& Space Sci.* 46, 975
Skorov, Yu.V. & Rickman, H. 1999, *Planet.& Space Sci.* 47, 935